**Final Report for NASA Grant # NNX09AI14A**

**PROJECT TITLE:**
Investigation of Ablation and Spallation-Enhanced Radiative Heating Predictions using DPLR

---


COLLABORATOR FOR NASA-AMES RESEARCH CENTER:

Michael J. Wright
(Name)
NASA Ames Research Center
(Address)
Mail Stop 230-2
Moffett Field, CA 94035-1000
650-604-4210
(Phone)
650-604-0350
(Fax)
michael.j.wright@nasa.gov
(Email)

COLLABORATOR FOR PARTICIPATING INSTITUTION:

Stephen M. Ruffin
(Name)
Georgia Institute of Technology
(Address)
School of Aerospace Engineering
Atlanta, GA 30332-0150
404-894-8200
(Phone)
404-894-2760
(Fax)
stephen.ruffin@ae.gatech.edu
(Email)


**AUTHORIZED REPRESENTATIVE FOR PARTICIPATING INSTITUTION**

Ms. Janis Goddard
(Typed Name)

Contracting Officer (and Manager, Other Federal Programs)
(Title)

Office of Sponsored Programs
Georgia Institute of Technology
Atlanta, GA 30332-0420
(Address)

**PROJECT TITLE:**
Investigation of Ablation and Spallation-Enhanced Radiative Heating Predictions using DPLR

## ABSTRACT

The radiative heating environment encountered during a high-speed reentry poses a unique problem for the design of thermal protection systems (TPS). The radiation heat flux reaching a body is the result of a complex interplay of many different systems. The emission of radiation is a strong function of the temperature and the species composition present in the shock layer, and in turn, the energy exchange due to the radiation affects the fluid mechanics and chemistry. Ablation and spallation of the surface of the body further influence these factors.

This project extended the capability of the NASA Ames flow solver Data-Parallel Line Relaxation (DPLR) to model the effects of material response (ablation and spallation) on the radiative heating environment. Ablation-induced turbulence is a well-understood phenomenon and has been implemented by others. However, the effects of radiation caused by the increased diffusion of carbonaceous species into the shock later will be studied. Additionally, the effect of spalled particles in the shock layer on radiative heating was investigated. The work has resulted in advancement of this important capability and joint publication of two AIAA papers by the investigators at Georgia Tech and at NASA Ames.

## OVERVIEW AND SUMMARY OF RESEARCH PROJECT

As NASA embarks on a greater number of planetary missions, the requirements put forth for affective, yet lightweight thermal protection systems (TPS) intensify. The material must be substantial enough to ensure the survival of the payload and crew during the reentry phase of the mission, but lightweight enough to be put into space at a reasonable cost. A result of the material's light weight and the violent conditions encountered during entry, the material begins to degrade, which introduces a new unknown into what is already a complex, highly coupled problem.

The primary objective of this effort is to develop accurate predictions of the aerothermal loads encountered during such an entry, which is critical in aiding the design of TPS materials. Only through accurate prediction, measurement, and validation can the required confidence in TPS design be achieved. As materials such as phenolic-impregnated carbon ablator (PICA), first used in NASA's Stardust mission, come into greater use, the ability to predict the ablation radiation environment will be important in these designs. This work also extends the capability of the Data-Parallel Line Relaxation (DPLR) tool, in use at NASA.

DPLR has emerged as the primary Navier-Stokes CFD tool for TPS analysis by NASA Ames due to its demonstrated accuracy, efficiency and its inclusion of much of the relevant physics for TPS analysis. DPLR is an MPI-based parallel flow solver that has been used extensively in reentry flow analysis. The current project is a follow-on to a prior funded effort and in the current work the previous DPLR-NEQAIR coupling efforts were extended to model the effects of ablation and spallation. This validated model will have significant benefit, for not only lunar and Mars return missions, but any entry in which ablative TPS systems are used in a radiating environment.

The secondary objective of the proposed work was to use the newly developed capability as an explanation for unexplained discrepancies between the heating predictions for past missions, such as Galileo and Pioneer, and the measured recession rates of their TPS.

Throughout this effort, a close collaborative effort with NASA Ames personnel was maintained for detailed planning, modification and updates. This collaboration included periodic teleconferences with all parties involved. This effort also involved two 10-week duration onsite stays during the Georgia Tech summer semester. This work resulted in joint publication between NASA and Georgia Tech personnel involved in this collaboration took place. The references for these publications are shown below:

1. Pace, A., Bose, D., Ruffin, S.M., "A Loosely-Coupled Approach for Shock-Layer Radiation Modeling in DPLR," AIAA Paper 2009-4312.

2. Pace, A., Ruffin, S.M., and Barnhardt, M., "A Coupled Approach for Predicting Radiation Attenuation in Particle-Laced Flows," AIAA 2011-3771, June, 2011.

The second publication has been submitted for subsequent Journal publication as well. The capability enhancement provided by this collaborative effort will be of substantial benefit to those conducting TPS studies including radiative and convective heat transfer analysis of critical CEV and planetary entry missions. In addition, this effort met important student educational objectives and enhanced ties and interest with the talent pool at Georgia Tech.

## DETAILED DESCRIPTION OF RESEARCH PROJECT

### Nomenclature

| | | |
|---|---|---|
| $\rho$ | = | density |
| c | = | particle separation distance |
| $\lambda$ | = | wavelength |
| $C_D$ | = | drag coefficient |
| $C_v$ | = | specific heat |
| $e^o$ | = | internal energy at zero Kelvin |
| $E$ | = | total internal energy |
| $F,G$ | = | flux in x-,y-direction |
| $k$ | = | (subscript) particle bin number |
| $K_H$ | = | heat transfer coefficient |
| $M$ | = | Mach number |
| $n$ | = | particle number density |
| $r$ | = | particle radius |
| $Re$ | = | Reynolds number |
| $S$ | = | particle frontal area ($=\pi r^2$) |
| $T$ | = | temperature |
| $U$ | = | state vector |
| $u$ | = | velocity in x-direction |
| $v$ | = | velocity in y-direction |

## I. Introduction and Motivation

PARTICLE-laced flows are of engineering importance in a number of disciplines. These include, but are not limited to, the flows associated with rocket nozzles, combustors, turbomachinery, and thermal protection systems [1]. In recent years, analysis of these flows have even included investigations of Martian and Lunar dust.

As a reentry vehicle enters an atmosphere, the hot gases behind the strong shock wave create an extreme heating environment around the vehicle. Development of thermal protection systems (TPS) has ensured the survival of payload and crew, and has allowed the exploration of even more extreme environments. Ablating heat shields have had success by, instead of the heat shield absorbing the heat of reentry, carrying the energy away in the form of pyrolosis gases. An associated phenomena with ablation is spallation, wherein instead of gas leaving the surface of the TPS, the material breaks apart into typically micron-sized particles, which then advect downstream [2,3].

It is desired to determine the effect, if any, the presence of spallation particles has on the reentry heating environment. As particles move downstream and into the shock layer, they heat up, carrying energy away with them and away from the heat shield. Conversely, eddies created by the movement of particles through the flow can increase mixing between the shock layer and boundary layer, increasing the heating at the surface.

More interestingly, the presence of spalled particles can also influence the radiative heating environment. A cloud of particles at the surface could reflect, scatter, and absorb radiation before it reaches the surface. Also, heated particles in the shock layer could emit radiation downstream, heating areas that ordinarily would not undergo such a heat load.

The goal of this effort is to develop a coupled spallation particle model within an existing computational fluid dynamics (CFD) code, in this case, the Data-Parallel Line Relaxation (DPLR) [4] code developed and maintained at NASA Ames Research Center. Once the model is developed and verified, it will be used to study the effect of spallation on the radiative heating environment.

Past studies have sought to simulate mixed fluid-particle flows. Most efforts resemble those used to compute mixed-phase flows. Perrell, Candler, et. al, used an Eulerian methodology [5] to model condensation of water particles in the expanding section of a combustion-heated hypersonic wind tunnel. This approach also used discrete bin sizes to differentiate particle sizes. Parrell later applied the methodology to a continuous distribution of particles [6] (dispensing with size bins) using a probability-

density function (PDF) approach. However, this approach was only applicable in one dimension. Later studies would be performed using a variety of approaches and continuum flow solvers.

An experiment was performed in the Interaction Heating Facility (IHF) at NASA Ames Research Center by George Raiche and David Driver. The experiment measured spectroscopic emission in the shock layer in front of ablating and non-ablating material samples at a range of heating conditions. The goal of the experiment was to observe whether the emission spectra was affected by the contribution of radiating ablation products in the shock layer. The experiment did see some unexpected results, however. Figures 1 and 2 show the emission spectra obtained in the experiment.

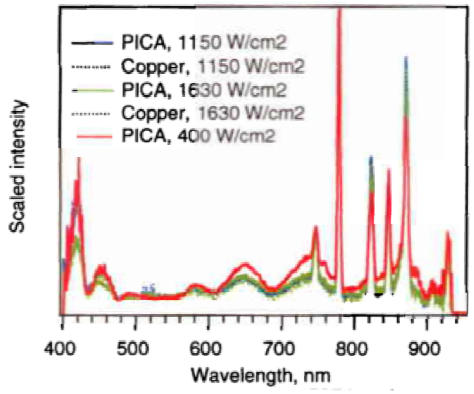


**Figure 1. Emission spectra from IHF test.** Note that the emission at higher heating hates shows lower intensity in some wavelength ranges. The intensity of some peaks is also affected.

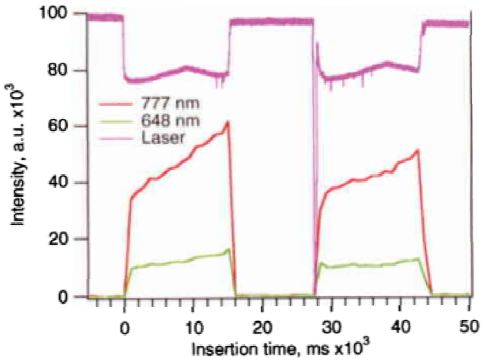


**Figure 2. Spectroscopic intensity over time in IHF test.** Note the decrease in intensity during the second insertion.

The experiment showed some unexpected results. In Figure 1, the test with the lowest surface heating rate (400 W/cm$^2$, in red) shows a higher emission intensity in some wavelength regions, such as in the 650-750nm range, the than the higher heating tests. Additionally, the test with the highest surface heating (1630 W/cm$^2$, in green) experiences lower emission peaks (namely at 420, 840, and 880nm) than tests with lower heating rates. Looking at emission intensity versus time for the same IHF test (Figure 2), shows that emission at a later time in the test (where the sample has experienced a longer duration of heating) is lower than the emission measured earlier in the test.

Raiche and Driver speculated that the inconsistency in the emission spectra could be attributed to the presence of spalled particles in the shock layer. It is believed that spalled particles could affect the radiative heating environment. Particles could scatter, absorb, or reflect (attenuate) radiation, resulting in differences

in the spectra. Higher surface heating would result in a greater production of spallation products in the shock layer. This was presented as a possible explanation for the decrease in emission in the higher heating case seen in Figure 1. Additionally, as a sample is heated for a longer duration, the surface breaks down, resulting in more ablation and spallation products. This is a possible explanation for the decrease in emission seen later in the test as seen in Figure 2.

## II. Methodology

### A. Description of Particle Flow

Previous efforts to model particle-laced flows have either chosen to model the particle phase though a Lagrangian or an Eulerian forumation. The Lagrangian formulation computes and tracks the dynamics of individual particle in the flow, using simple mechanics. This formulation is simpler; computing a particle's trajectory in the flow is an easy task given the size and mass of each particle, and a model for which to describe the forces acting on it. It has the disadvantage of being more difficult to define time-averaged quantities. It is also more computationally expensive for large numbers of particles. In the Eulerian formulation, the particle field is treated as continuum, similar to a fluid. While this is different than the true physical nature of the particle field, it lends it self better for computing time- and space-averaged quantities. It is also more computationally efficient for large numbers of particles. For these reasons, the present effort will model the particle using an Eulerian approach.

An additional drawback of the Eulerian approach is its difficulty in handling different sized particles. In this effort, particles of different sizes are separated into individual "bins", and solved independently, as if they were different species in the flow. The governing equations for the particle cloud in two dimensions become:

$$\frac{\partial \vec{U}_k}{\partial t} + \frac{\partial \vec{F}_k}{\partial x} + \frac{\partial \vec{G}_k}{\partial y} = \vec{W}_k \tag{1}$$

Where:

$$\vec{U}_k = \rho_p n_k V_k \begin{bmatrix} 1 \\ u_k \\ v_k \\ e_k \end{bmatrix} \tag{2}$$

$$e_k = C_{v_p} T_k + e_k^o + \frac{u_k^2 + v_k^2}{2} \tag{3}$$

The subscript $k$ indicates that the equation applies for the particles in the $k$th size bin. The fluxes $F$ and $G$ are simply the state vector $U$ multiplied by the corresponding component of velocity. These equations resemble the Euler equations in fluid mechanics, with the absence of the pressure term in the flux expressions. The physical defense for this is, as the particle cloud is not truly a continuum fluid, there is assumed limited interaction between the particles, negating the need for a pressure term. The extension to three dimensions is apparent.

Coupling with the Navier-Stokes solver (DPLR) occurs through the source term vector, $W$. The source terms represent interaction of the particles with the main flow through drag and heat transfer. The drag terms are as follows:

$$W_{k_2} = n_k \frac{1}{2} C_D \rho (u - u_k)^2 S_k \tag{4}$$

$$W_{k_3} = n_k \frac{1}{2} C_D \rho (v - v_k)^2 S_k \tag{5}$$

The choice of the model of drag coefficient has to be chosen to be consistent with the flow regime in the specific problem. For the case of TPS spallation in the hypersonic flow environment, the drag coefficient model of Carlson and Hoglund [17] was chosen:

$$C_D = \frac{24}{\mathrm{Re}} \frac{\left[1 + 0.15\,\mathrm{Re}^{0.687}\right]\left[1 + \exp\left(-\frac{0.427}{M^{4.63}} - \frac{3}{\mathrm{Re}^{0.88}}\right)\right]}{1 + \frac{M}{\mathrm{Re}}\left[3.82 + 1.28\exp\left(-1.25\frac{\mathrm{Re}}{M}\right)\right]} \tag{6}$$

Which represents Stokes drag (applicable for low Reynolds number), with a Mach and Reynolds number correction. In this case, *Re* represents the Reynolds number based upon vectoral relative velocity.

The energy source term is made up of two components. The first represents work done on the fluid due to particle drag:

$$W_{k_4,drag} = W_{k_2,drag} \cdot u_k + W_{k_3,drag} \cdot v_k \tag{7}$$

The second component is due to heat transfer:

$$W_{k_4,conv} = \frac{3\kappa K_H U_{k_1}}{r_k^2 \rho_p}\left(T - T_k\right) \tag{8}$$

Where the expression for the heat transfer coefficient is taken from Carlson and Hoglund:

$$K_H = \frac{1}{2}\frac{2 + 0.459\,\mathrm{Re}^{0.55}}{1 + 3.42\frac{M}{\mathrm{Re}}\left(2 + 0.459\,\mathrm{Re}^{0.55}\right)} \tag{9}$$

Fluxes are extrapolated using a first-order upwind scheme. While this method is inherently dissipative, particle clouds are by their very nature diffuse; in this case, the numerical error is consistent with the physics of the problem.

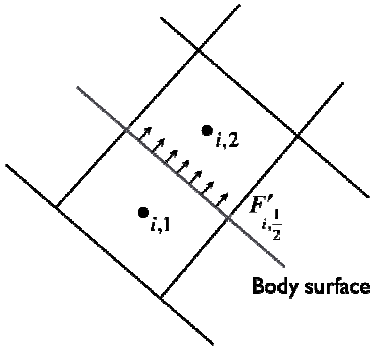


**Figure 3. Visualization of the computational mesh at the body surface.**

### B. Boundary Conditions

The boundary conditions for the spallation particle field resemble those for an inviscid, supersonic flow. At walls where spallation is present, the boundary conditions are a blowing wall. For a given problem, the size, mass, number density, and speed of the particles being ejected from the surface are defined, and are usually based on empirical models or more sophisticated surface response models. The temperature of the particles is taken to be the surface temperature computed in the Navier-Stokes solution. Thus, given these parameters, the density at the surface can be computed:

$$\rho^{wall} = \left(\frac{\text{\# particles}}{\text{volume}}\right)\left(\frac{\text{mass}}{\text{particle}}\right) \tag{10}$$

Thus the flux at the surface is simply defined as:

$$F'_{i,\frac{1}{2}} = \begin{bmatrix} \rho_{blow} u_{blow} \\ \rho_{blow} u_{blow}^2 s'_x \\ \rho_{blow} u_{blow}^2 s'_y \\ e_{blow} u_{blow} \end{bmatrix} \tag{11}$$

Walls where particles are not being emitted are treated as inviscid walls (flow tangency). While this can lead to inaccuracies in some cases (to be explained in Section D), in most applications it proves to be a valid assumption. As there is no pressure term in the momentum fluxes, information does not travel the domain in the same manner as a traditional fluid; information does not travel upstream. Thus, at the exit boundaries of the flow domain are treated as if they are supersonic exit boundaries, and the flow properties in the boundary cells are obtained through a first-order extrapolation.

**C. Solution Methodology**

Coupling between the Navier-Stokes equations and the particle phase can be accomplished by two means, a monolithic- or loose-coupling scheme. In a monolithic-coupled scheme, the conservation equations for each bin of the particle phase are solved directly with the reacting Navier-Stokes equations. The source terms of momentum and energy (described earlier) are cross terms in a large matrix. While the monolithic-coupled scheme provides the greatest accuracy and stability, it is inefficient and computationally expensive. If solving the reacting Navier-Stokes equations resulted in inverting an NxN matrix, the resulting system with the particle phase is (N+4k)x(N+4k), for *k* size bins in a two-dimensional simulation. The inefficiency is compounded by the fact that, since the only coupling occurs via the momentum and energy source terms, this matrix is largely sparce.

Instead, a loose-coupling method is used to advance both the main flow and the spalled particles. An initial flow solution is obtained (without particles) in DPLR. Next, the particle flow is advanced at the boundary for one iteration, and the updated information about the particle field is used to compute the source terms for the Navier-Stokes solution in DPLR. These source terms are added in the next DPLR calculation, and the main flow is advanced one iteration. The updated flow solution is used to calculate the updated source terms, which are then used in the next particle iteration. The process is then repeated until steady state, with special consideration for time stepping and stability.

**D. System Stability**

The coupled fluid-particle system experiences unique stability concerns. With the lack of a pressure term in the momentum fluxes, it is impossible to define a speed of information propagation (sound). Thus, it is not possible to define a stability requirement in a traditional sense (such as the CFL requirement). This problem was also encountered by past efforts to model particle flows (Perrell, et. al.). In the present study, the choice of time step is related to the propagation speed of the particle flow itself, thus the time step becomes:

$$\Delta t \leq \frac{\Delta x}{u_{part}} \tag{12}$$

Here, Δx is defined as the minimum grid spacing in the domain. Additionally, it was observed (as it was in past studies) that in some cases, excessive particle densities could occur along wall surfaces. This is a side effect of the momentum averaging used in the Eulerian formulation. In the Eulerian formulation, a control volume has an average momentum; information regarding the distribution and direction of individual particles is lost. In most regions of the flow, where the particles tend to track with the main flow, this is not an issue for stability, nor is it a hindrance to obtaining an accurate solution. Near a wall, however, particles are moving toward the surface, tracking with the flow, and (more importantly) some are reflecting off. By performing the Eulerian averaging, this reflection information is lost. Without this reflection mechanism in place, the result can be (in some cases) unexpectedly high densities along surfaces. This effect is not observed for smaller particles, where the effective drag acting on the particle is higher, due to the larger surface area to volume ratio. As the drag is higher, these particles tend to track with the fluid more so than larger ones. The result is the particles being carried away with the flow before having the opportunity to collude at the wall surface.

**E. Particle Blackbody Emission and Attenuation**

The presence of spalled particles in the shock layer affects the radiation heating environment in two ways. First, as particles are heated, and their temperature increases, they begin to emit radiation. The result is an incident blackbody spectrum that contributes to the overall spectrum observed in the test. Spectroscopic calculations in this effort are calculated using the NASA Ames code NEQAIR [19].

The Nonequilibrium Air Radiation (NEQAIR) code is a line-by-line radiation code developed at NASA Ames. It computes the emission and absorption spectra (along a line-of-sight) for atomic species, molecular species electronic band systems, and infrared band systems. Radiative heating rate is determined using either a tangent slab or spherical cap assumption. Individual electronic transitions are evaluated for atomic and molecular species. The code can model the bound-free and free-free continuum radiation caused by interactions of electrons with neutral and ionized atomic species. The external inputs required by NEQAIR are the (nonequilibrium) temperatures and species number densities along a line-of-sight. For the radiation calculations used in this analysis, these data are received from a DPLR flow computation.

When NEQAIR is solved along a line of sight, the resulting calculation gives both the spectroscopic intensity as well as the total radiation heat transfer at every point along the line. As was stated previously, the two expected contributions to the spectral data are blackbody emission due to heated particles, as well as attenuation do to scattering, blocking, and absorption. Instead of directly adding these models into NEQAIR, an approximate method was developed to compute these properties. We start with a simplified version of the radiative transfer equation:

$$\frac{dI}{dx} = I_0(T,\lambda) - \alpha I \tag{13}$$

The term on the left-hand side of the equation represents the change in the spectroscopic intensity along a given one-dimensional line. For the purposes of this analysis, this line is the same as the line of sight used in the NEQAIR calculation.

The first term on the right-hand side of the RTE represents the contribution to the radiative intensity due to blackbody emission of radiation. The blackbody contribution to the spectrum is then added at each point, and summed along the line-of-sight to find the total contribution:

$$I(r,\lambda) = 4\pi r_{part}^2 \frac{2hc^2}{\lambda^5} \frac{1}{e^{\frac{hc}{\lambda kT}} - 1} \tag{14}$$

Here $T$ represents the computed particle temperature. It should be noted that in addition to being a function of the particle temperature, it is also a function of the particle radius. A particle with a larger radius has a larger contribution to the emission spectra, since radiation is emitted over a larger surface area. The blackbody function is also dependent on wavelength. For this effort, as the RTE is integrated along the line of sight, the blackbody contribution from each particle is summed for all particles, and for all wavelengths.

The second term on the right-hand side of the RTE represents the decrease in radiative intensity, in this case due to scattering and absorption. The scattering, reflection, and absorption (attenuation) of radiation by a field of particles is a well-known and quantitative phenomenon. However, it is nonetheless a complex calculation that is dependant on such factors as particle size, wavelength of the incident radiation, material properties, as well as the direction of incoming radiation. As a result, the actual form of this term can get quite complicated. A common simplification to this term is shown in Equation 13. It is assumed that the decrease in spectroscopic intensity is proportional to the incoming intensity, where the proportionality constant, α, is referred to as the extinction coefficient.

An initial approximation is made to calculate this extinction coefficient. In his analysis [2], Park made the assumption that incoming radiation is completely absorbed or reflected by particles that are in a given control volume. These particles affectively cast a “shadow” behind them (Figure 4), which is projected on the rear side of the volume. The shadowed area due to a single particle is equal to the frontal surface area of that particle. The contribution due to all particles is assumed to be the sum of all the surface areas of all the particles in the volume.

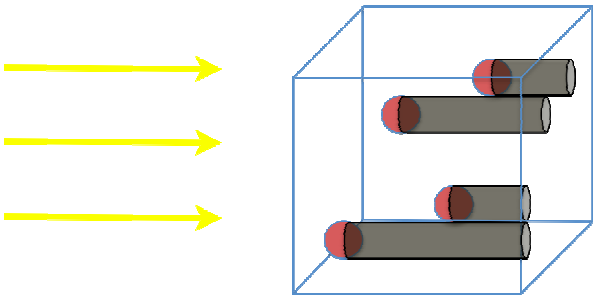

**Figure 4. Diagram showing particle shadows**

While the above method is simple, as it only depends on geometric optics, it is desired for this work to arrive at a more accurate and less crude approximation. General scattering models that are applicable to all regimes of scattering by particles are difficult to arrive at, and often require the solution to Maxwell's Equations. However, one can arrive at less complicated solutions by making assumptions about the scope of the problem. Two important parameters in particle scattering theory are known as the size parameter, $x$, and the clearance-to-wavelength ratio, $f$. These parameters are defined as such:

$$x = \frac{2\pi r_{part}}{\lambda} \tag{15}$$

$$f = \frac{c}{\lambda} \tag{16}$$

Most applications relevant for TPS and heat transfer involve relatively diffuse clouds with large separation distances between individual particles ($f$ >0.5) [8], and thus the scattering can be called "independent", meaning that the scattering effect of a single particle does not depend on the presence of other particles in the cloud. Several well-known theories exist for the scattering effects of a single sphere, such as Rayleigh, Rayleig-Gans, and Mie scattering. Additionally, if only micron-scale particles are considered (which are particle sizes considered relevant to TPS spallation [14]), and if the wavelength regime is limited to those predominant in aerothermal heating applications, then the resulting size parameter is of order one. This size parameter is too large to employ models such as Rayleigh scattering, but is within the range of applicability of Mie scattering. As such, it is desired to develop and test a Mie scattering model and observe its effects on the attenuation of shock-layer radiation.

## III. Results

### A. Particle Flow Verification

The goal of this effort is to develop a coupled Navier-Stokes-particle flow solver. The results of the solution will be used to evaluate the impact the particles have on the radiative heating environment. The results of Raiche and Driver's experiment in the NASA Ames Interaction Heating Facility (IHF) will be used as a comparison. The exact spallation rate (in other words, the particle size, number density, and velocity) is not known a priori, and thus is is not possible to make an exact comparison. Instead, what this analysis seeks to determine is, by varying these parameters (namely particle size and the speed at which they are expelled from the surface), what effects the presence of the spallation products has on the emitted spectra.

The first step is to simply vary these parameters, and qualitatively assess the behavior of the coupled system. First, a converged DPLR solution for the IHF. Figure 5 shows a detailed view of the computational mesh around the test sample.

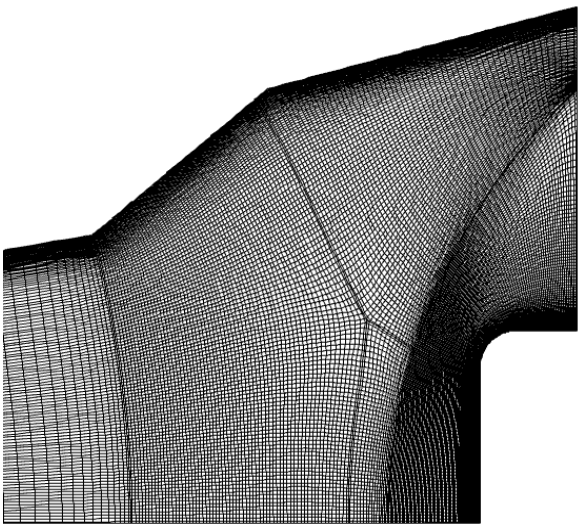

**Figure 5. Detail view of computational mesh**.

Next, the spallation model was applied to the IHF case. For each simulation, a particle number density of 1000 particles/cm$^2$ and a velocity of 50 m/s was chosen to be the surface condition. The first case shown below involves a mean particle radius of 1.5x10$^{-5}$ m particles. This is a larger size than expected for a TPS spallation case, but it was chosen simply to observe the behavior of the system. Figure 6 shows contours of particle mass fraction, defined as:

$$c_{part} = \frac{\rho_{part}}{\rho_{part} + \rho_{flow}} \tag{17}$$

As can be seen in the figure, particles are ejected from the surface, and become entrained in the flow. Particles emitted on the front of the test sample accelerate around the rounded corner of the sample, but continue on their own trajectory, not tracking with the fluid. This is because it is a larger-sized particle; the effective drag acting on it is lower because of the lower surface area to volume ratio. Particles emitted on the top of the sample are entrained in the boundary layer. The aforementioned collusion of particles at the surface is observed.

The simulation was repeated for a particle radius of 1.5x10-6 m, which is an order of magnitude smaller than in the previous simulation. A similar plot of mass fraction is shown in Figure 7. In this case, since the surface area to volume ratio is much higher for the smaller-sized particle, the effective drag acting on the particles is also higher. The result of this is that as particles are emitted from the front of the sample and become entrained in the flow, as they are accelerated around the corner, they track the fluid more closely than in the previous case. And as the particles are more easily entrained in the fluid, the high-density collusion on the top of the sample is not as apparent.

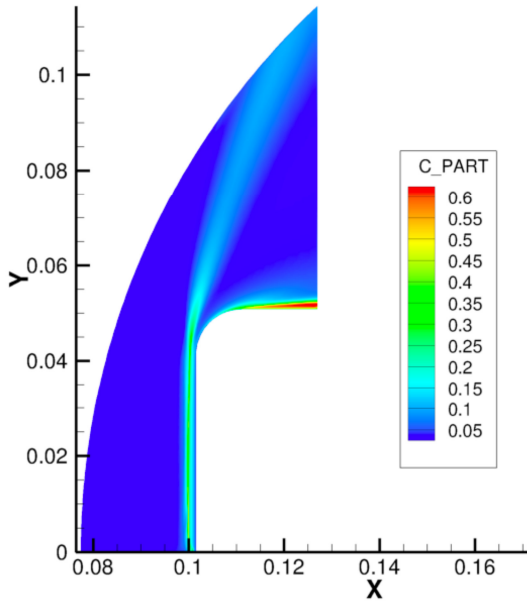


**Figure 6. Particle mass fraction in coupled a IHF simulation, $r_{part}=1.5x10^{-5}$ m.**

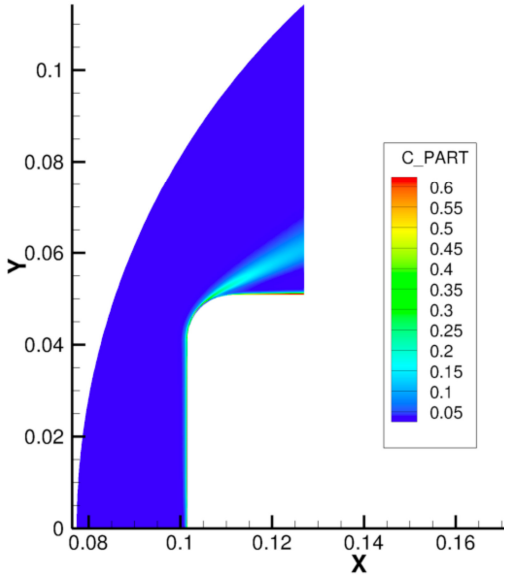


**Figure 7. Particle mass fraction in coupled a IHF simulation, $r_{part}=1.5x10^{-6}$ m.**

Next, particle radius and velocity were varied to qualitatively simulate another arc-jet case performed at Ames. Figure 8 shows the result of an experimental test of a PICA sample (left) and the result of a coupled simulation (right). PICA is the same material used in the Raiche and Driver IHF test. As the particles are heated and glow, they trace paths in the photograph. These are analogous and comparable to

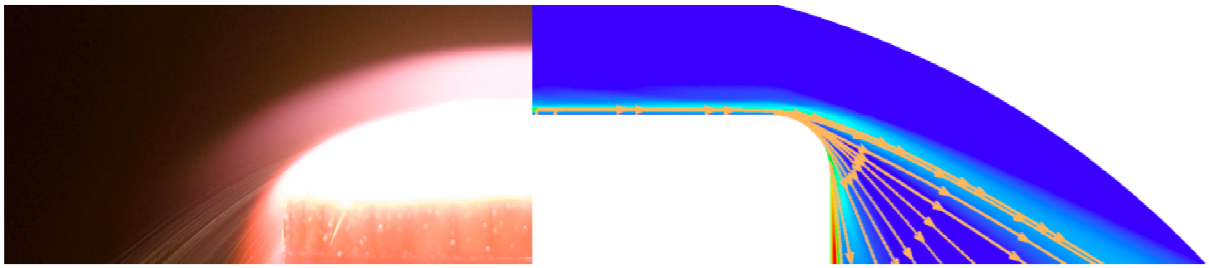

**Figure 8. Arc-jet experiment and simulation.** Visible are the results of the experiment (left), and simulation (right).

the streamtraces shown in the simulation.

## B. Spectroscopic Results

The aforementioned arcjet simulation was used as a baseline in order to perform a spectroscopic analysis of the shock-layer radiation. First, a line of sight was taken across the shock-layer, and used as an input to perform a NEQAIR calculation. The spectral systems considered in this analysis are shown below in Table 1. For atomic systems, bound-bound, bound-free, and free-free transitions were considered.

| **Spectral Systems** |
|---|
| Atomic O |
| Atomic N |
| $N_2$ 1- |
| $N_2$ 1+ |
| $N_2$ 2+ |
| NO β |
| NO γ |
| NO δ |
| $O_2$ SR |

**Table 1. Spectral Systems Considered**

The line of sight was run through NEQAIR across the 855.5-39,600Å wavelength range. However, only the visible spectrum is going to be displayed for visual clarity, and because it is relevant to the previous analysis. A preliminary spectrum is shown below:

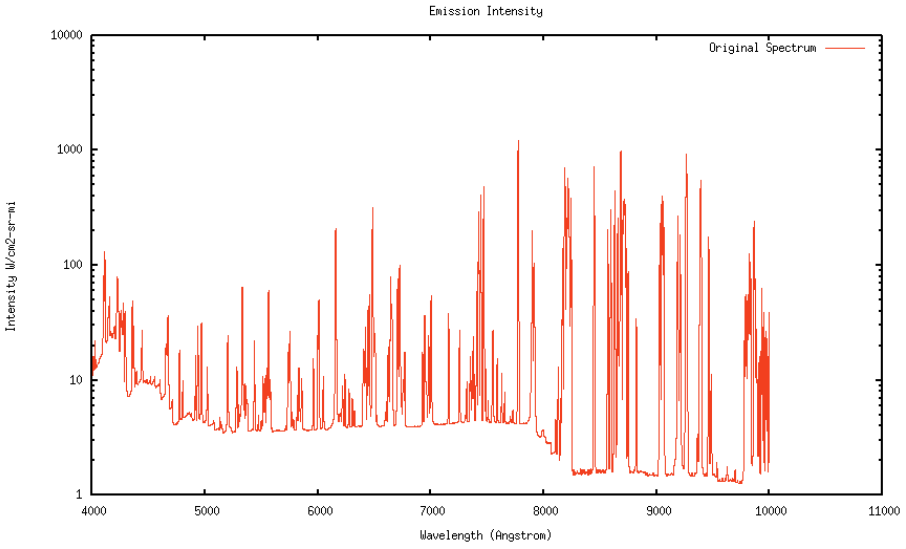


**Figure 9. Original Spectrum**

The spectrum is displayed in log-scale in order to make the molecular continuum radiation at lower wavelengths more visible. Next, the blackbody emission model was applied to the spectrum. Figure 10 shows the original spectrum with the blackbody contribution:

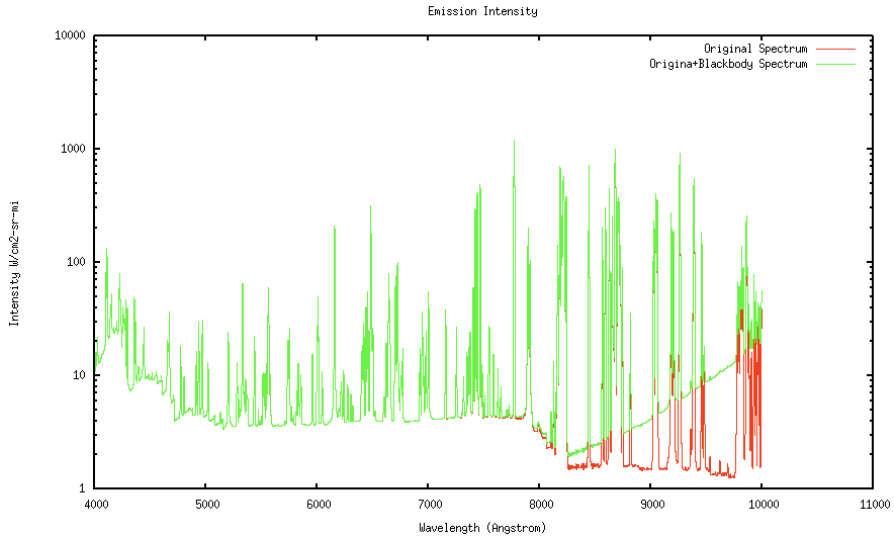


**Figure 10. Original Spectrum with Blackbody Contribution.**

At lower wavelengths, the contribution due to the blackbody emission by the particle cloud is negligible compared to the original shock-layer emission. At higher wavelengths however, the emission becomes more prevalent. At these wavelengths, while the blackbody emission is greater than the molecular continuum radiation, it is still far lower than the atomic emission peaks. As such, the magnitude of these peaks are relatively unaffected.

The next step is to apply the simplified Park attenuation model to the original spectrum. The results are shown in Figure 11. As the model is a simplified geometric optical model, it does not predict any variation in attenuation with wavelength, and so the reduction in spectral intensity is uniform across the spectrum.

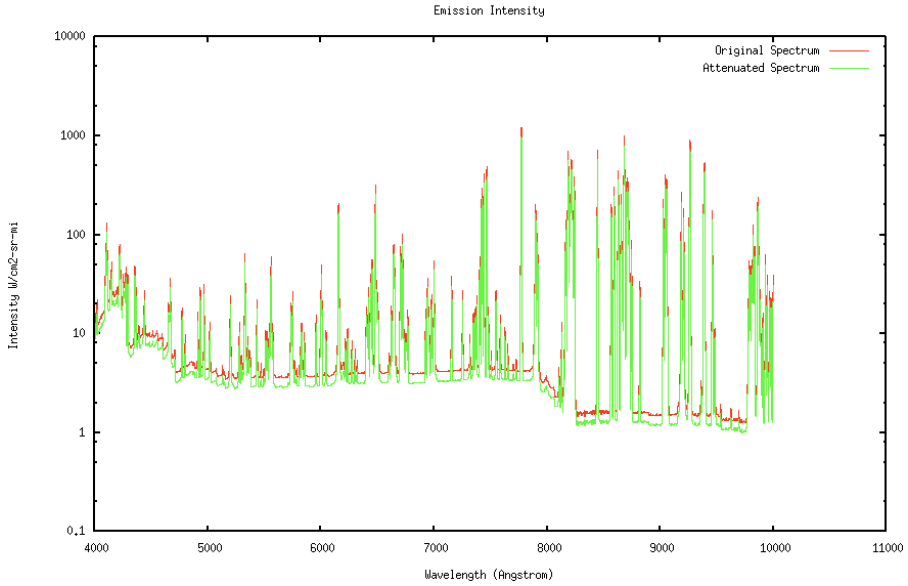


**Figure 11. Original and Attenuated Spectrum.**

Finally, a spectrum was computed that took into account both the effects of blackbody emission and attenuation:

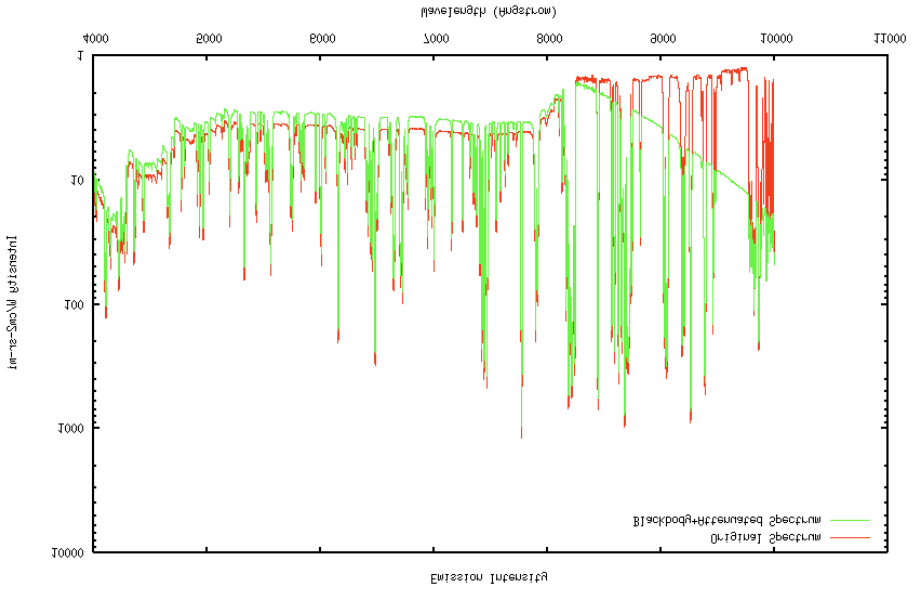


**Figure 12. Original and Attenuated Spectrum with Blackbody Emission.**

While a more rigorous scattering model needs to be developed, the current methodology demonstrates the capability to compute spectral attenuation due to the presence of spallation particles. Further development and testing is ongoing.

## IV. Conclusions and Future Work

A coupled Navier-Stokes/spallation particle methodology was developed, and preliminary testing showed satisfactory qualitative agreement with the expected trends. The blackbody emission, as well as a preliminary model for the scattering and absorption of radiation was developed. The tools were applied to a NASA Ames Arc-jet simulation in order to study the effects of scattering and emission due to spallation products. Further work includes more complete and quantitative analyses applying the methodology to a NASA Ames Interaction Heating Facility (IHF) test is continuing. Additionally, a more rigorous Mie scattering model will be developed and tested for this validation.

## V. References

[1] Mathieu, R. "Mechanical Spallation of Charring Ablators in Hyperthermal Environments." AIAA Journal. Vol. 2, No. 9.

[2] Park, C., et al. "Radiation of Spalled Particles in Shock Layers." Journal of Thermophysics and Heat Transfer. Vol. 18, No. 4.

[3] Park, C. "Interaction of Spalled Particles with Shock Layer Flow," AIAA-1999-0353, Reno, NV, January 1999.

[4] Wright, M. J., Candler, G. V., and Bose, D., "Data-Parallel Line Relaxation Method for the Navier-Stokes Equations," AIAA Journal, Vol. 36, No. 9, Nov. 1998, pp. 1603-1609.

[5] Perrell, E. "Two-Phase CFD Calculations with Continuous Distributions of Particle Sizes" AIAA -1998-3459

[6] Perrell, E and Candler, G. "Computation of Nonequilibrium Two-Phase Flows in a Combustion Heated Wind Tunnel." AIAA-1994-0774.

[7] Ekkad, S and Han, J. "Heat Transfer Distributions on a Cylinder with Simulated Thermal Barrier Coating Spallation." Journal of Thermophysics and Heat Transfer. Vol. 13, No. 1.

[8] Modest, M. "Radiation Heat Transfer," Academic Press, London, England, 2003.

[9] Raiche, G. and Driver, D. "Shock Layer Optical Attenuation and Emission Spectroscopy Measurements During Arc-Jet Testing with Ablating Models." AIAA-2004-825

[10] Potivsky, A, et al. "Dynamic of Plumes Generated by Local Injection of Ablated Material." AIAA-2008-577

[11] York, B.J, Lee, R.A., et al. "Progress in the Simulation of Particulate Interactions in Solid Propellant Rocket Exhausts." AIAA-2001-3590.

[12] Nussbaum, J. et al. "Numerical Simulation of Reactive Di-Phasic Particle Flow." AIAA 2007-4161.

[13] Sullivan, J.M., and Kobayahi, W.S., "Spallation Modeling in the Charring Material Thermal Response and Ablation (CMA) Computer Program." AIAA 1987-1516.

[14] Lundell, J.H., "Spallation of the Galileo Probe Heat Shield." AIAA 1982-0852.
[15] Davies, C.B. and Park, C. "Trajectories of Solid Particles Spalled from Carbonaceous Heat Shields." AIAA 1982-0200.
[16] Williams, A. et al. "Thermal Radiation Absorption by Particle-Seeded Gases." Journal of Spacecraft and Rockets, Vol. 8, No. 4, April 1971.
[17] Carlson, D.J., and Hoglund, R.F., "Particle Drag and Heat Transfer in Rocket Nozzles," AIAA J, vol. 2, no. 11, pp. 1980-1984, November 1964.
[18] Swain, C.E., "The Effect of Particle/Shock Layer Interaction on Reentry Vehicle Performance." AIAA 1975-734
[19] Whiting, E.E., Park, C., Liu, Y., Arnold, J.O., and Paterson, J.A., "NEQAIR96, Nonequilibrium and Equilibrium Radiative Transport and Spectra Program: User's Manual," NASA RP-1389, Dec. 1996.